Int. J. Pharm. Investigation, 2024; 14(1):212-224.
https://www.jpionline.org

Original Article

Preparation and Characterization of Hydroxyapatite-Chitosan Biocomposites of *Cissus quadrangularis* Linn. for Bone Regeneration in Osteoporosis

Tejas B Patel*, Shantilal P Padhiyar, Vipul T Prajapati, Vashisith P Bhavsar, Nishit D. Patel, Dharmik A. Shah

Faculty of Pharmacy, Dharamsinh Desai University, College Road, Nadiad, Gujarat, INDIA.

ABSTRACT

Background: This research was conducted to create a treatment for osteoporosis (bone degenerating disorder) with hormone replacement therapy using Hydroxyapatites and chitosan as a composite. The research aims to develop bio-composite hydroxyapatite/chitosan-drug composites that will improve the absorption of calcium and phosphorus ions into the bone by acting as an extra source of these nutrients. Hydroxyapatite which resembles to bone minerals composition was prepared using chemical reaction method later incorporating it with chitosan using co-precipitation method forming hydroxyapatite-chitosan composites. **Materials and Methods:** Finally synthesizing Hydroxyapatite/Chitosan-Drug composite using homogenous mixture kept for 12 hr for incorporation. The prepared Hydroxyapatite and hydroxyapatite/chitosan composites underwent XRD, FTIR and TGA studies giving us sharp diffraction peaks, functional group characteristic peaks and percentage weight loss respectively. **Results and Discussion:** Micrometrics measurements of the composites of hydroxyapatite and chitosan reveal good, Carr's index, percentage porosity and Hausner's ratio in batch F5 and F6 out of all six batches. HA/CS composites were also evaluated for water absorption study, water loss study, estimation of calcium and phosphorous ion. Estimation of phytogenic steroid and in-vitro drug release study was done on HA/CS-drug composites. **Conclusion:** As a conclusion, AFM study of batch F5 with drug revealed there was an improvement in uniformity of composite size and shape. The X drug was able to homogeneously incorporate in HA/CS composites giving good release of drug up to 12 hr. The study produced nano-composites, an innovative bone regeneration and tissue creation approach.

Keywords: Hydroxyapatite, Chitosan, Osteoporosis, Bone regeneration, Scaffolds.

Correspondence:
Dr. Tejas B Patel
Associate Professor, Faculty of Pharmacy, Dharmsinh Desai University, Nadiad-387001,Gujarat, INDIA.
Email: tejaspatel264@gmail.com

Received: 29-08-2023;
Revised: 03-10-2023;
Accepted: 03-11-2023.

INTRODUCTION

The Bone is renowned for its tenacity, adaptability, mechanisms for promoting growth, and capacity for self-repair and remodeling. Because of its distinct structure and mechanical qualities, it has even received significant attention from the materials engineering community.[1] The skeleton is made up of a complex network of bones that serves as a framework for the musculoskeletal system's movement as well as a means of protecting the body's important organs.[2] The bone itself is made up of three levels of hierarchical architecture:[1] the nanostructure, which is made up of fibrillary collagen, non-collagenous organic proteins, and embedded mineral crystals;[2] the microstructure, which is made up of the Haversian system, lamella, and osteon;[3] the macrostructure, which consists of cortical and cancellous bone.[3] The ability to endure physiological demands without breaking depends on both the form of individual bones and the tissue qualities of the bone as a whole. Additionally, bone serves as a storehouse for a variety of vital minerals, including calcium and phosphate, and it is crucial in the control of ion concentrations in extracellular fluid.[2] Various methods are available to overcome bone defects when undergoing medical operations for damage related to the bones. 10% of the bone grafting are done by using synthetic graft substitutes. Autografts are the next method; in this case, tissues are obtained from the same patient, although there are drawbacks, such as donor site morbidity and pain after grafting. On the other hand, allografts are bone graft replacements obtained from another patient, which carry a risk of infection during the transplantation process along with an inflammatory response that could result in graft rejection.[4,5] The transplanting of cells from various species is another type of xenograft. Now let's talk about biomaterials, which include synthetic graft replacements made of polymers, ceramics, metals, bioactive glasses, and composite materials. Metals used as grafts provide stress shielding, which weakens the host tissue and makes

DOI: 10.5530/ijpi.14.1.27

it more brittle. There are several solutions, but they all have problems, necessitating the creation of a substrate that improves rebuilding while restoring the function of damaged tissue.[6] The advantage of avoiding repeated surgery at the donor site is undoubtedly a draw for the tissue engineering strategy. The designed scaffold will deliver three-dimensional tissue, offering the best vascularization and growing conditions.[6] A desirable scaffold would be biocompatible, non-immunogenic, have a linked porous network to allow cell penetration and the transfer of nutrients, oxygen, and waste products, have enough surface area, and have a variety of end terminals to encourage the movement of cells, association, distinctions, and proliferation.[7,8] Our scaffolds must meet important criteria for bone tissue engineering, including biological compatibility, suitable mechanical properties, regulated degradation rate, suitable pore dimension and morphology, suitable surface chemistry, porousness, osteoconductivity, and osteoinductivity.[9] The ceramic phosphate of calcium substance hydroxyapatite continues to hold the most potential for bone tissue engineering. It has demonstrated significant osteoconductivity, biocompatibility, and bone-bonding properties, and both its chemical structure and content match those of the mineral that makes up genuine bone.[10] In contrast to other calcium phosphates, hydroxyapatite is thermodynamically stable at physiological pH and does not solubilize under physiological conditions. Already, bone tissue damage is filled, extended, and repaired with it.[11] Chitosan is a promising candidate for the repair of cartilage abnormalities as it is also biocompatible with the GAG that is naturally present in cartilage. Chitosan has been investigated for use in a variety of biomedical applications, such as space-filling implants, systems to deliver drugs, and dressings for wounds, it has received Food and Drug Administration approval for use in these applications. With minimal or no fibrous encapsulation, this substance causes the least amount of foreign body reaction. This unique biopolymer, which shares a number of chemical and structural similarities with collagen, degrades more quickly than bio-ceramics. As a result, adding hydroxyapatite to the chitosan polymer matrix will improve osteoconductivity and biodegradability while also substantially improving its mechanical strength.[12,13]

The aim of this research was to create a HA/CS composite that included a formulation that increased the absorption of calcium and phosphorus ions into bone as an extra source.

A great deal of focus is currently focused to plants that are traditionally used as botanical remedies as potential therapeutic agents for bone tissue engineering. The powerful medicinal plant *Cissus quadrangularis* Linn. (CQ) is well-known for its own osteogenic capabilities. A popular perennial succulent climber plant in the Vitaceae family is called Cissus quadrangularis. The plant is known as "Hadjod" or "Asthisamharaka" in India and is well-known as a treatment for problems with the bones, muscles, and ligaments. The stem is the most often used portion, while nearly every aerial and subsurface part has therapeutic potential. Numerous compounds, including carbohydrates, proteins, phenol carboxylic acids, triterpenoids, phytosterols, glycosides, saponins, vitamin C, and alkaloids have been identified in studies on the phytochemical makeup of the plant. These plants also have plenty of calcium in them.

MATERIALS AND METHODS

Calcium hydroxide, Orthophosphoric acid, Ammonium hydroxide, Sodium chloride, Dipotassium hydrogen phosphate, Calcium chlorides were received from SDFCL. Chitosan was provided from Himedia, Potassium chloride, Sodium bicarbonate Magnesium chloride, Hydrochloric acid, Sodium sulfate, Sulfuric acid, Ammonium molybdate was received from Sulab and Calcium Kit was received from Aspen lab.

Preparation of Hydroxyapatites

Hydroxyapatites were prepared using chemical reaction method. 18 g of $Ca(OH)_2$ dissolved in 130 mL of distilled water (solution 150 mL of distilled water with 10 mL of H_3PO_4 dissolved in it (solution 2). Drop by drop, solution 2 was incorporated with solution 1. After applying NH_4OH to sustain the mixture's pH at 10.5 for 48 hr, the finished product was allowed to ripen. The pure form of Hydroxyapatite (HA) is obtained by filtering the solution and drying it at 110°C in a hot air oven.[14-16]

Preparation of Hydroxyapatite (HA)/ Chitosan (CS) composites via co-precipitation method

Co-precipitation was used to create HA/CA composites100 mL of acetic acid was required to dissolve 1 g of chitosan at a 1% ratio (solution 1). 100 mL of distilled water was used to dissolve 1 g of 1% hydroxyapatites in order to make solution 2. Drop by drop, the other 2 solution was combined with solution 1. The mixture was stirred at 45°C for 15 min. In order to keep the mixture's pH at 11, an ammonia solution was used. HA/CS composites are produced when the solution turns opalescent.[17,18]

Preparation of HA/CS-Drug composites

HA/CS-Drug composites was prepared using homogeneous mixture and the formulation composition of the composites were depicted in Table 1. In distilled water (solution 1), HA/CS composite was dispersed. In (solution 2), the drug was dissolved in distilled water. Solution 2 was drop wise added in to solution 1. The combination was kept for 12 hr for incorporation of drug in to HA/CS composites. Filter the solution and dry at 50° C, which give the HA/CS- Drug composites.[19]

Preparation of stimulated body fluid (SBF)

SBF was prepared following Kokubo's technique. The following are the ion concentrations (in g): NaCl (8.035 g), $NaHCO_3$ (0.335 g), KCl (0.255 g), $.3H_2O$ (0.231 g), $MgCl_2.6H_2O$ (0.311 g), 1M HCL (38 mL), $CaCl_2.2H_2O$ (0.3675 g), $NaSO_4.10H_2O$

(0.071 g), and $NH_2C($ (Tris buffer, 6.118 g). In accordance with the prescribed procedure, the reagents were attenuated in 800 mL of distilled water at 36.58°C with continuous stirring. With distilled water, the total amount was increased to 890 mL, and the temperature was then raised to 36.58°C and 1M HCl was used to balance the pH to 7.4. 1 L of water that was distilled was added along with the solution's final volume. SBF must be consumed within 30 days of preparation and kept in the refrigerator (5-10 C).[20]

Estimation of Phytogenic Steroid in Herbal Extract

Estimation of phytogenic steroid was done by using UV double beam spectrometry. A 10 mg medication that had been precisely measured was transferred to a 10 mL volumetric glass flask and dissolved with Stimulated Body Fluid (SBF) to obtain a standard stock solution (1 mg/mL). Different dilutions to stock solution were made to obtain at various concentrations of 50, 100, 150, 200, and 250 µg/mL.[21]

Characterization and Evaluation of HA/CS-Drug composites

Fourier-transform infrared spectroscopy (FTIR)

Batch F1, F2, F3 hydroxyapatite and chitosan were analyzed using FTIR. The Grams, Buck scientific model-500 with KBr as the background was used to acquire the data. The samples are put within the sample holder, and the diffuse reflectance technique is used to examine the characteristic peaks.[22,23]

X-ray Diffraction (XRD)

Amorphous medication dosage and physical state changes are also investigated using XRD. The XRD studies of bulk hydroxyapatites, chitosan composites F1 to F6 and HA/CS- Drug were carried out using XRD (Bruker AXS GmbH, Karlsruhe, Germany).[24,25]

Thermo Gravimetric Analysis (TGA)

A technique for examining modifications to a material's mass that occur in accordance with predefined temperature variations is called Thermo-Gravimetric Analysis (TGA). A few of the processes that could change the mass are decomposition, sublimation, vaporization, adsorption, degradation, desorption, oxidation, and reduction. Utilizing TGA (Mettler), research on F1, F3, F5, and hydroxyapatites was conducted.[26]

Atomic Force Microscopy

The measurement was taken with a NT-MDT integrated solution for nanotechnology. The corresponding relative altitude maps were measured using silicon probes (NT-MDT) with a nominal spring constant while tapping in the air. Using the Root Mean Square (RMS) of the height distribution, the roughness was assessed from the AFM images to determine the lowest indentation depth that could be used in the tests.[27]

Composite size

The typical microscope should be able to measure particle sizes between 0.2 and roughly 100 m using optical microscopy. Composites are placed on a slide or riled cell and set on a mechanical stage in accordance with the microscopic approach. A micrometer that can be used to measure particle size is attached to the microscopic eyepiece. A photograph from which a slide is made and displayed on a screen for assessment which can be used, or the field can be projected onto a screen to make it easier to measure the particles.[28]

Angle of Repose

The flow attribute of solids has been described in terms of angle of repose. An aspect of interparticulate friction or the resistance to movement in composites is called angle of repose. The cone-like pile of material created by this process assumes a constant, three-dimensional angle as its angle of response. The funnel's height, which determines how composites move through it, can either be set in relation to the base or it can change as the pile grows.[27]

$$\tan(\alpha) = \text{height}/0.5\text{base}$$

Where, α is Angle of Response.

Bulk Density

Bulk density, which is measured in g/mL, is the composites' ratio to the bulk volume it fills. The volume of the composites, which weighs 5 g, was measured by pouring it into a 100 mL measuring cylinder and weighing it again.[29]

Mass of composites/volume of packing equals bulk density.

Table 1: Formulation of HA/CS composites.

Batch	HA (Weight %)	CS (Weight %)
F1	30	70
F2	40	60
F3	50	50
F4	60	40
F5	70	30
F6	80	20

Tapped Density[27,29]

To calculate the tapped density, 5 g of the composites were precisely weighed, placed in a 100 mL measuring cylinder, and the volume of it was recorded. Mechanical tapping was used to generate a bulk volume of 100 times the constant volume of the real volume of the composites and the void space between the composites.

Tapped density=Mass of composites/Tapped volume of packing

Hausner Ratio

The Hausner ratio of beads can be calculated through comparing the tapped density to the bulk density by employing the equation.[30]

Hausner's ratio=Tapped density/Bulk density

Carr's Index

The % compressibility of the beads was determined using Carr's compressibility index.[27-30]

Carr's index (%)=tapped density-Bulk density/Tapped density*100

Percentage Porosity

The porosity and density were determined using a liquid displacement method by employing ethanol as the displacement liquid, which can easily flow across the pores of the composite materials and does not lead to shrinkage or swelling as a non-solvent of the polymers. A sample weighing W was placed within a graduated cylinder that held a predetermined amount (V1) of ethanol. Forcing the ethanol into the pores of the composite, the sample was held in the ethanol for 5 min before going through a series of quick evacuation-depressurization cycles. The cycle was repeated until no more air bubbles were visible coming from the composites. Then, V2 was calculated as the sum of the ethanol and ethanol-impregnated scaffold volumes. The volume of the skeleton of the HA/CS composites made up the volume difference (V2-V1). The ethanol-impregnated composites were taken out of the cylinder, and V3 was measured as the volume of remaining ethanol. The composites' porosity of the open pores, was determined using.[27-30]

$$\epsilon=(V1-V3)/(V2-V3)$$

Percentage Water Absorption

To assess water absorption, each sample was weighed before being dipped into distilled water at 37°C. After being immersed in the medium for varying durations of time, the samples were carefully removed, gently squeezed between two filter papers to eliminate any remaining water, and weighed on an exact scale. The following equation is used to compute the water absorption capacity (%).[30,31]

$$\text{Water absorption (\%)} = W_f\text{-}W_i/W_i*100$$

Where, the sample's starting weight is w_i, and its final weight, w_f, is determined by immersion. To ensure the data, the test was run on three samples, and the average result was obtained.

Percentage Weight Loss/ Biodegradation

The weight of the composites was reduced *in vitro* by incubating them in SBF for a variety of times-1, 3, 7, 15, 21, and 28 days-at pH 7.4 and 37°C. The composites were periodically taken from the mixture and overnight at 50°C dried. The subsequent equation was used to compute the weight loss:[29,31]

$$\text{Weight loss (\%)} = W_0\text{-}W_t/W_0*100$$

The sample's starting weight is w_o, and its weight at time (t) is w_t. Three samples were used in each experiment, and the average value was taken to ensure the results.

Calcium and Phosphorus Ions Estimation

The SBF solution and solid composites were assessed prior to and following varied immersion times. Notations and composition of the HA/CS composites. In order to test the bioactivity, the composites were submerged in SBF for varied lengths of time up to 8 days at pH 7.4 and body temperature (37°C). The SBF has a composition similar to that of human blood plasma and is frequently used for *in vitro* studies. Following the immersion time, the solutions were measured for phosphorus and calcium ion concentrations at 318 and 437 nm, respectively, using a spectrophotometer. The tests were carried out three times for each, and the results were verified using the average value.[31,32]

RESULTS

X-ray Diffraction (XRD) Study of Prepared HA

XRD spectra of prepared hydroxyapatite were presented in Figure 1(a). It indicated that the sharp diffraction characteristic peaks that appeared at around 31.8° and 25.9° correspond to the speaks of HA (31.773° and 25.879°). Figure 1 showed XRD spectra of pure hydroxyapatite, XRD spectra of prepared hydroxyapatite was as identical as pure hydroxyapatite. This indicated prepared hydroxyapatite in pure form.

Fourier-transform Infrared Spectroscopy (FTIR) study of Prepared Hydroxyapatites

FTIR of hydroxyapatite is presented in Figure 2(a). Characteristic peaks of water molecules, amine I, carbonate, and phosphate was detected in spectra of HA. The absorption band at 3540 and 3487 cm^{-1} correspond to the stretching of the lattice OH- ions, whereas the absorbed water band appeared at 3287, 3163 and 1648 cm^{-1}. The characteristic band of HPO_4^{2-} was assigned at 1133 and 1064 cm^{-1}. An FTIR spectrum of pure HA is presented in Figure 2(b). Figure 2 (a) and (b) depicts the Fourier transform infrared

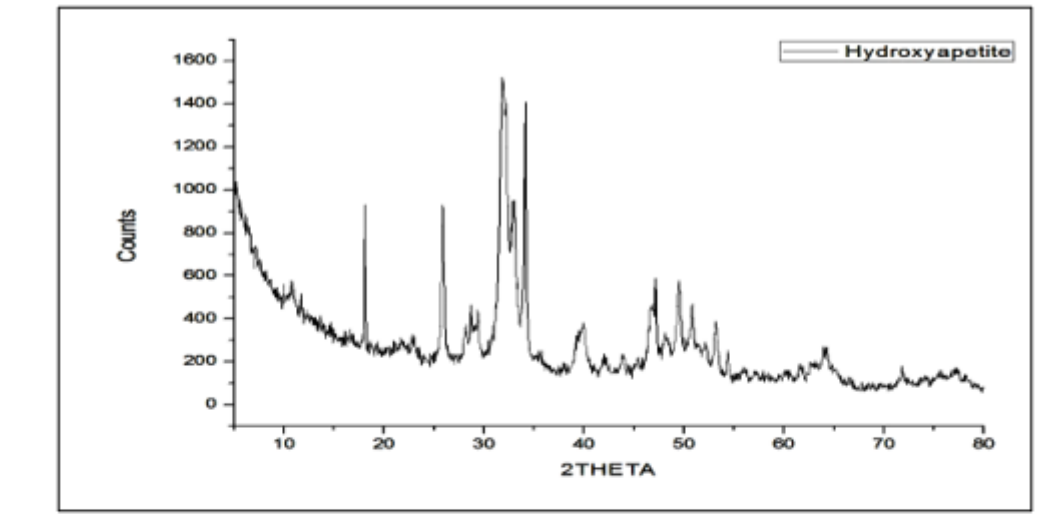

(a)

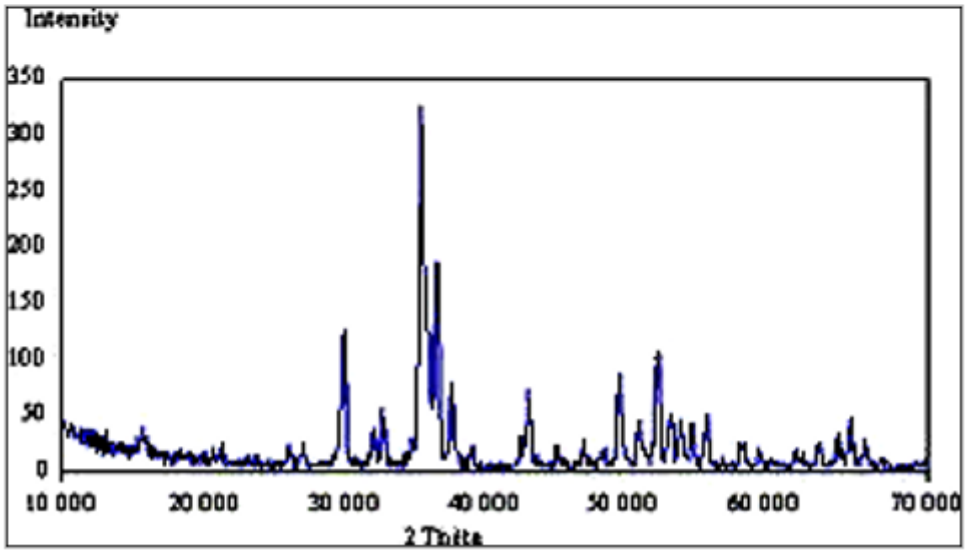

(b)

Figure 1: XRD study of (a) prepared HA and (b) pure HA.

spectrum of prepared and pure HA. Hence, prepared HA was in pure form.

Fourier-transform infrared spectroscopy (FTIR) study of prepared HA/CS composites

Figure 3 depicts a summary of the FTIR spectrum of the HA/CS composites. All of the HA and CS characteristic peaks were seen in the HA/CS composites. The peaks at 3570, 3420, 2920, 1720, 1640, 1280, 1030-960, 630, 602-560 cm^{-1} were tasked with stretching OH, OH of water, OH and CH, C=O, absorbed water/amide I, CCO, stretching PO_4^{3-}, liberational OH and bending PO_4^{3-}group, respectively. This indicated that the interaction between HA and CS was missing in HA/CS composites.

X-ray diffraction (XRD) study of prepared HA/CS composites

Figure 4 depicts the XRD patterns of HA/CS composites, chitosan, and HA. While HA was recognized by the acute diffraction characteristic peaks that appeared at around 31.8° and 25.9° (31.773°, 25.879°), chitosan was recognized by the broad peak that arose at 20° (20.305°, 21.290°). The characteristics of the peak for HA/CS composites with varied HA: CS ratios (30:70, 50:50, and 70:30) are shown in Figures 4(c), (d), and (e), respectively. This indicated the formation of composites.

Thermo Gravimetric Analysis (TGA) study

Figure 5 showed % weight loss of HA and HA/CS composites using TGA. % weight loss of Batch F1, F3, F5 and prepared HA

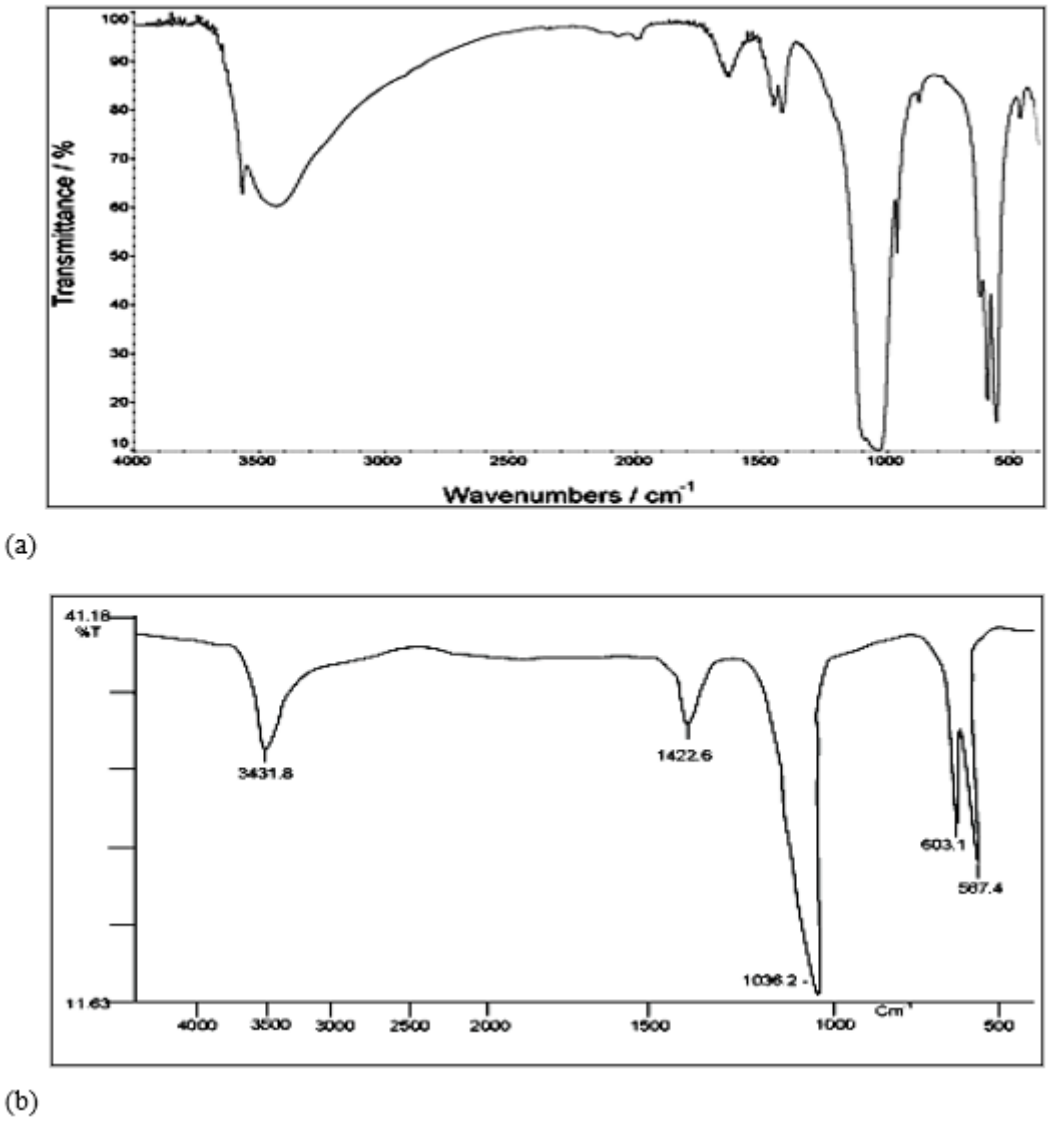

Figure 2: FTIR spectra of (a) prepared HA and (b) pure HA.

was 54.72 %, 53.00%, 34.38% and 41.93%, respectively. Batch F5 had low weight loss compared with other Batch F1 and F3. Hence, it had high binding affinity of HA toward the chitosan.

Physicochemical Characteristics of HA/CS composites

Results of micrometrics properties of HA/CS composites were showed in Table 2. It showed Mean composites size of batch F5 (3.892) and F6 (3.891) have a smallest composite size compared to other batches. Batches F1-F6's flow properties included angle of repose, Carr's index, and Hausner's ratio. Batches F5 and F6 had the lowest repose values of 22.06% and 22.08%, respectively. The Hausner's ratio and Carr's index of F5 and F6 revealed a strong association across all six batches. Results of % porosity indicated Batch F5 had high % porosity (26.53) compared to all 6 Batches.

Atomic Force Microscopy (AFM) study

Figure 6 showed the AFM of HA/CS composites (Batch F5). Which showed the minimum and maximum composite size was 0 and 101.834 nm, respectively. Mean composite size was 26 nm, Average roughness was 9.412 nm and Root Mean Square was 12.322 nm.

Percentage Water Absorption Study

The hydrophilicity of the chitosan polymer matrix is one among the most important features to examine when assessing the biomaterial for bone tissue engineering since it is essential for physiological fluid absorption and the transfer of cell nutrients and metabolites. With an increase in chitosan content, the ratio of water absorption ability rose continuously. According to the study, the HA/CS composites absorbed % of the water after 1, 3, 7, 15, 21, and 28 days. Chitosan's capacity to create reversible gel is what caused the findings that were seen. A higher CS content

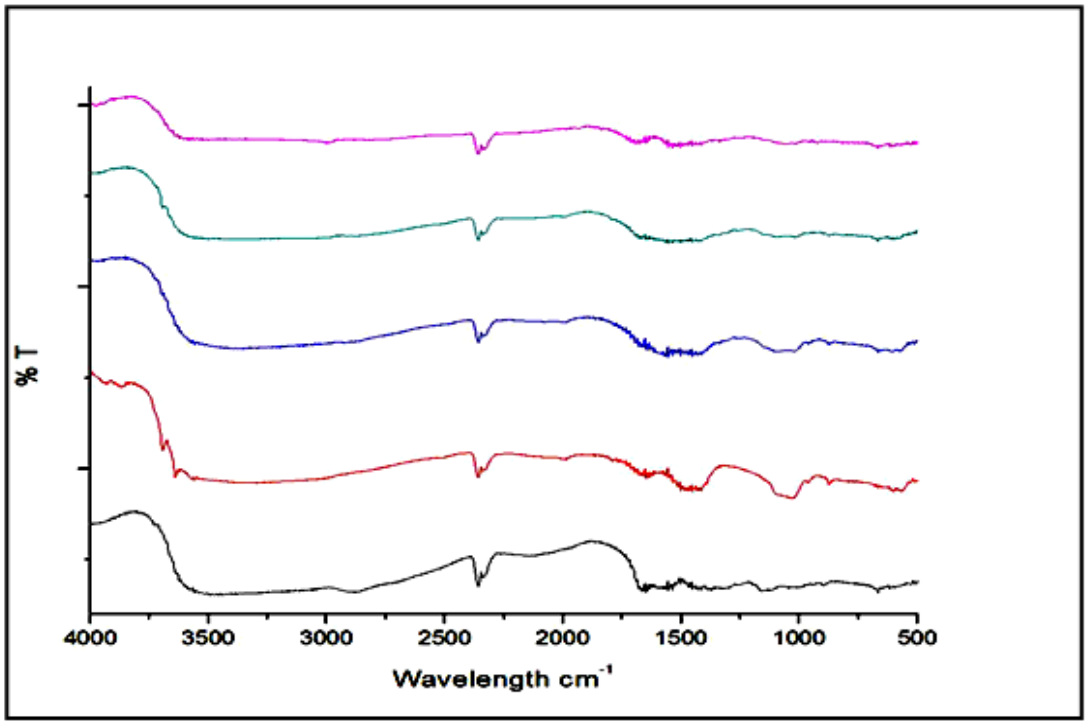

Figure 3: FTIR spectra of HA/CS composites.

in the HA/CS mixture reduces the weight fraction of HA. As a result, the batch F5% F6 had smaller amounts of CS 30% and 20%, respectively, and as a result, had greater water absorption ability. As a result, the addition of CS increased the OH group in the composite, increasing the hydrophilicity of the HA/CS composites. Chitosan integration enhanced the hydrophilic surface, which is good for cell attachment and proliferation. In comparison to other batches, batch F5 has a high capacity to absorb water, as shown in Figure 7.

Percentage Weight Loss/Biodegradation Study

Figure 8 displayed how the HA/CS composites fared in terms of weight reduction when compared to HA. Weight loss for batches F1 to F6 was lower than it was for other composites due to the composites' gradually declining chitosan concentration. Batch F1 contained a high level of CS (70%) and a low content of HA,[30] which caused the composite to degrade rapidly. The fact that the weight loss of batches F5 and F6 was lower than that of HA suggests that chitosan and HA interacted through their functional groups, resulting in the composites' high stability and reduced degradation.

Estimation of Calcium Ion

Figure 9 illustrated the concentration of calcium ions in batches F1 to F6 of HA/CS composites, control samples, and HA. after 1, 3, 5, and 8 days in SBF, respectively. After 8 days, all produced composites had lower calcium ion concentrations than pure HA and the control (SBF). This demonstrated the deposition of calcium Ca^{2+} ions on composite surfaces. This may be the result of Ca^{2+} interacting with the functional group of the chitosan polymer. Due to the rapid hydrolysis of the chitosan macromolecule chain in the presence of water, the composites with a high chitosan content in Stimulated Body Fluid (SBF) degraded more quickly. The findings also indicated that adding CS to the HA/CS composites improved the calcium ion absorption. This demonstrated the creation of a chitosan gel that is insoluble in water when calcium ions are present. As a result, it helps the CS polymer's osteogenic activity pharmacologically.

Estimation of Phosphorus Ion

Figure 10 showed that the concentration of PO_4^{3-} ions in SBF after immersion of pure HA and HA/CS composites. The estimation of PO_4^{3-} was compared with SBF as control. The results indicated the lower value of PO_4^{3-} ion in post immersion of HA/CS composites (F1 to F6) in SBF after 1, 3, 5 and 8 days (Table 3). This could be because chitosan has a strong affinity for phosphorus ions. In contrast to the control deposition of PO_4^{3-} ions the batch on the material's surface F5's lower values for PO_4^{3-} ion concentration. If sufficient chitosan is present, the amino groups that hydrogen bind with phosphorous ions in SBF might increase. Lower values were found for the PO_4^{3-} ion concentration after HA immersion.

By comparing the concentrations of Ca^{2+} and PO_4^{3-} ions in SBF for post immersing of Batches F1-F6.

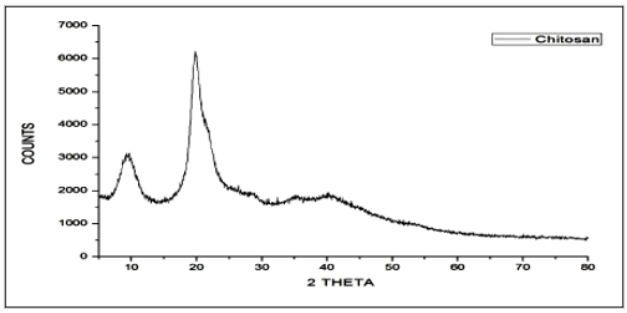

(a)

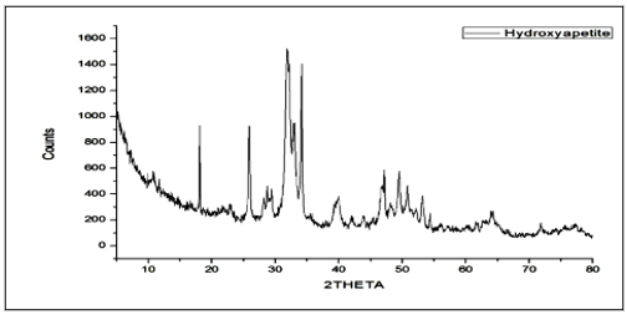

(b)

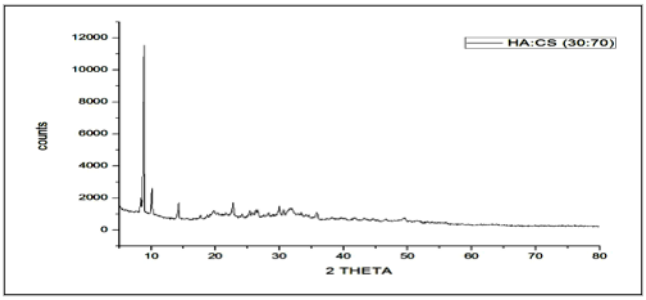

(c)

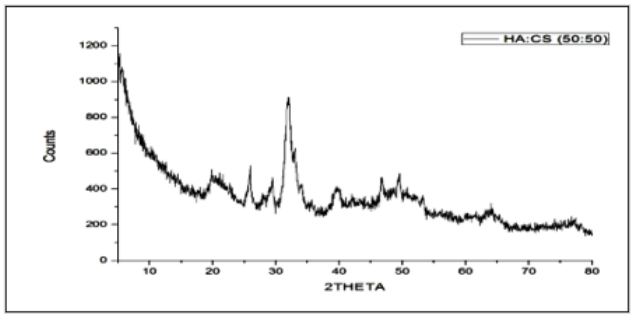

(d)

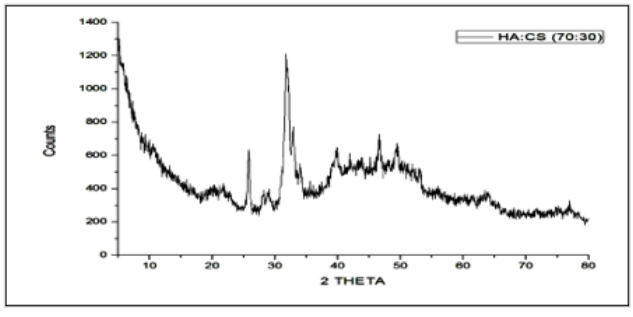

(e)

Figure 4: XRD of (a) Chitosan (b) HA (c) Batch F1 (d) Batch F3 and (e) Batch F5.

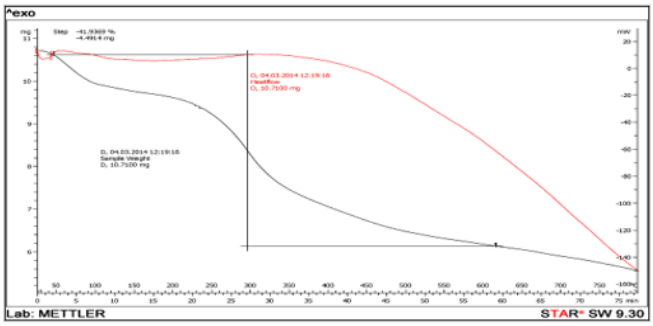

(a)

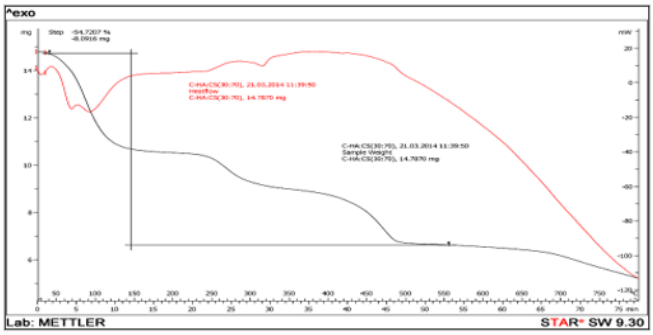

(b)

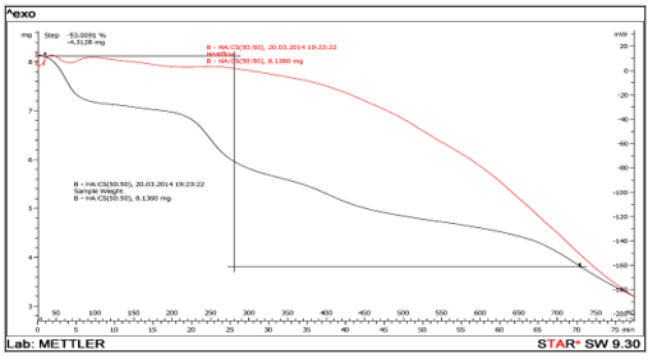

(c)

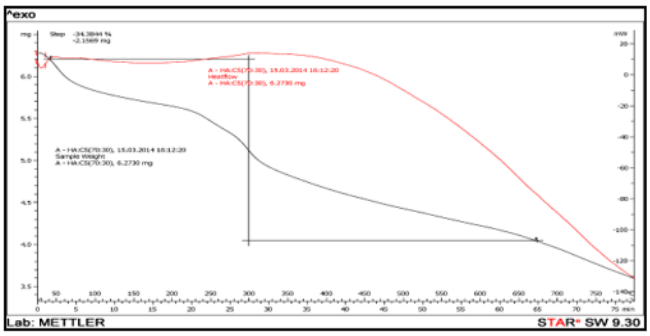

(d)

Figure 5: TGA of (a) prepared HA (b) Batch F1 (c) Batch F3 and (d) Batch F5.

Estimation of Phytogenic Steroid

Phytogenic steroid concentration was estimated in the extract of drug using UV- visible spectrophotometry at 268 nm λ max in Stimulated Body Fluid (Figure 10).

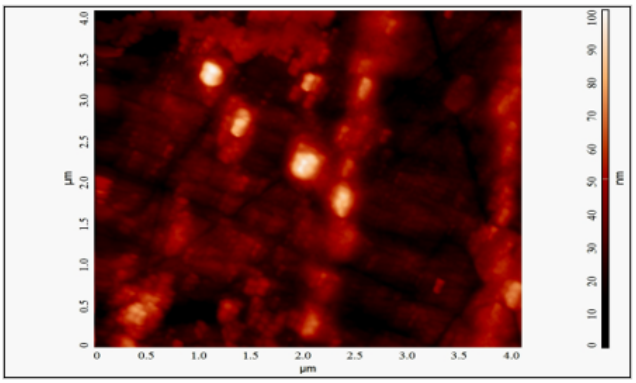

(a)

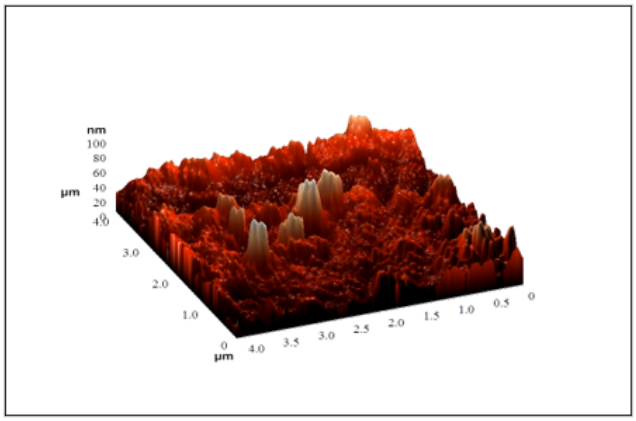

(b)

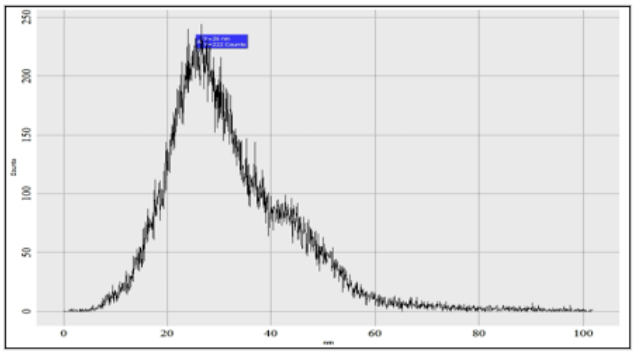

(c)

Max 101.834 nm.
Min 0 nm.
Peak-to-peak, Sy101.834 nm.
Ten-point height, Sz51.3636 nm.
Mean composite size: 26 nm.
Average 32.0837 nm.
Average Roughness, Sa9.41255 nm.
Root Mean Square, Sq 12.3228 nm.

Figure 6: AFM study of (a) 2D image of Batch F5 (b) 3D image of Batch F5 and (c) Histogram of Batch F5.

In vitro Drug Release Study of HA/CS-Drug Composites

Figure 11 depicts the *in vitro* drug release results from the HA/CS combination (Batch F1 to F6). A 12 hr drug release was visible in every composite. Also assessed was the amount of drug released

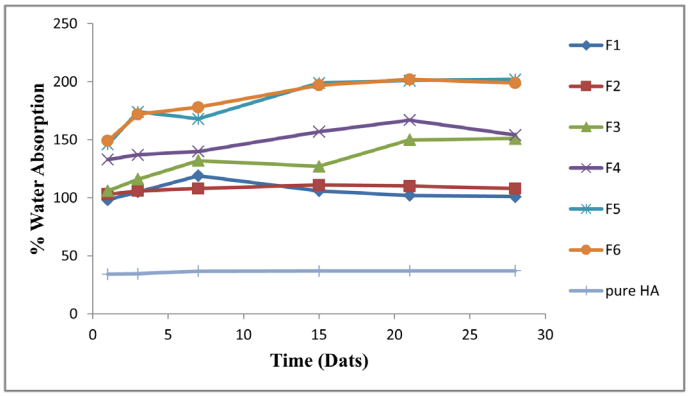

Figure 7: %Water absorption study of HA/CS composites.

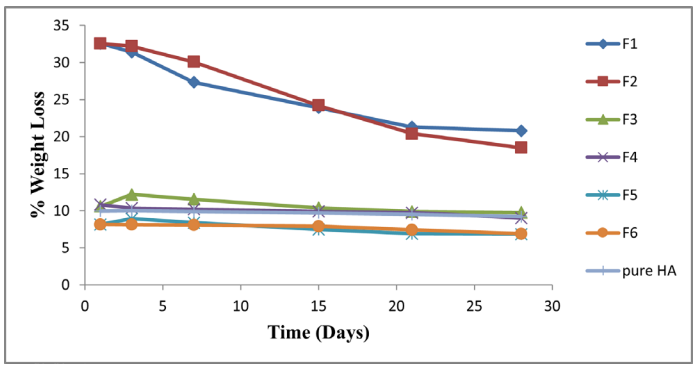

Figure 8: % Weight loss study of HA/CS composites.

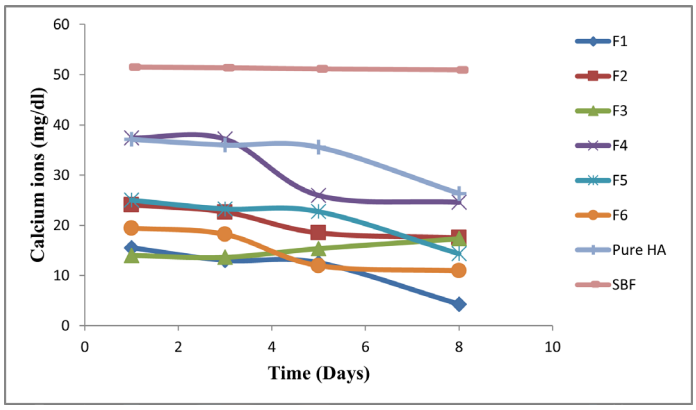

Figure 9: Estimation of calcium ions (mg/dl) in SBF.

from the HA-Drug and CS-Drug composites. After 12 hr, it revealed a medication release of over 70%. Within 6 hr, the pure drug released virtually all of its whole amount. The results of the study showed that drug release might be prolonged for up to 12 hr. HA/CS composites that include Drugs (Figure 11). After 12 hr, Batch F5 had a nearly 92.32% drug release. across all batches. In order to better characterize HA/CS-Drug composites, Batch F5 was chosen.

Fourier-transform infrared spectroscopy (FTIR) study of HA/CS-Drug optimized batch

Figure 12 showed the FTIR spectra of pure Drug and HA/CS-Drug (Batch F5) composite. All characteristic peaks of pure

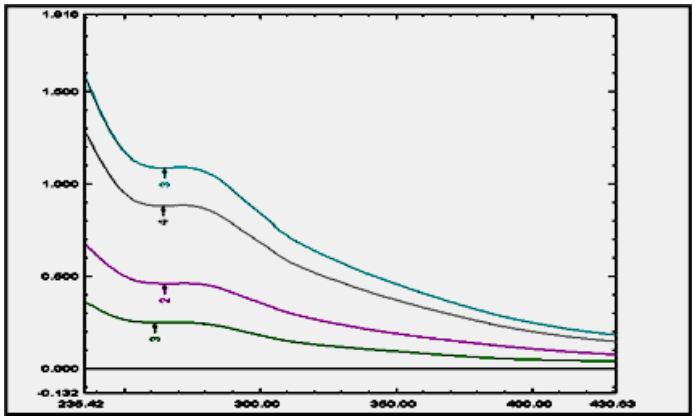

Figure 10: Estimation of λ max of phytogenic steroid.

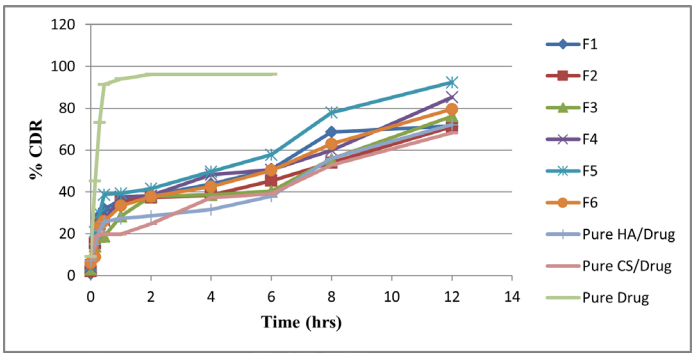

Figure 11: *In vitro* drug release study (% CDR).

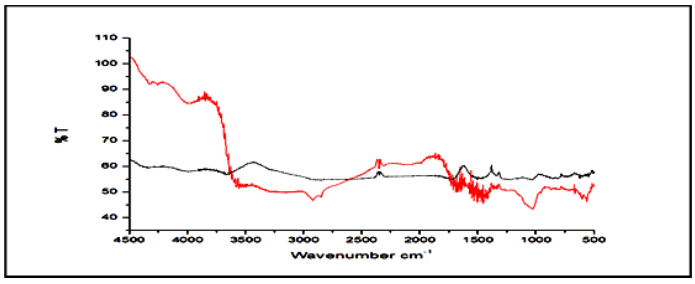

Figure 12: FTIR spectra of drug and batch 5.

Drug were observed in spectra of Batch F5. Which proved the Drug has properly incorporated in the HA/CS and there was no drug interaction between HA/CS and Drug.

Atomic force microscopy (AFM) study of Optimized batch

Figure 13 showed the AFM data of Batch F5 with drug composite. Which showed the minimum and maximum composite size was 0 and 137.71 nm, respectively. Mean composite size was 29.4 nm, Average roughness was 8.273 nm and Root Mean Square was 12.147 nm.

The results of AFM study revealed that the after incorporation of drug in HA/CS composite the uniformity of composite size and shape was improved and had uniform shape of HA/CS-Drug composite (Batch F5).

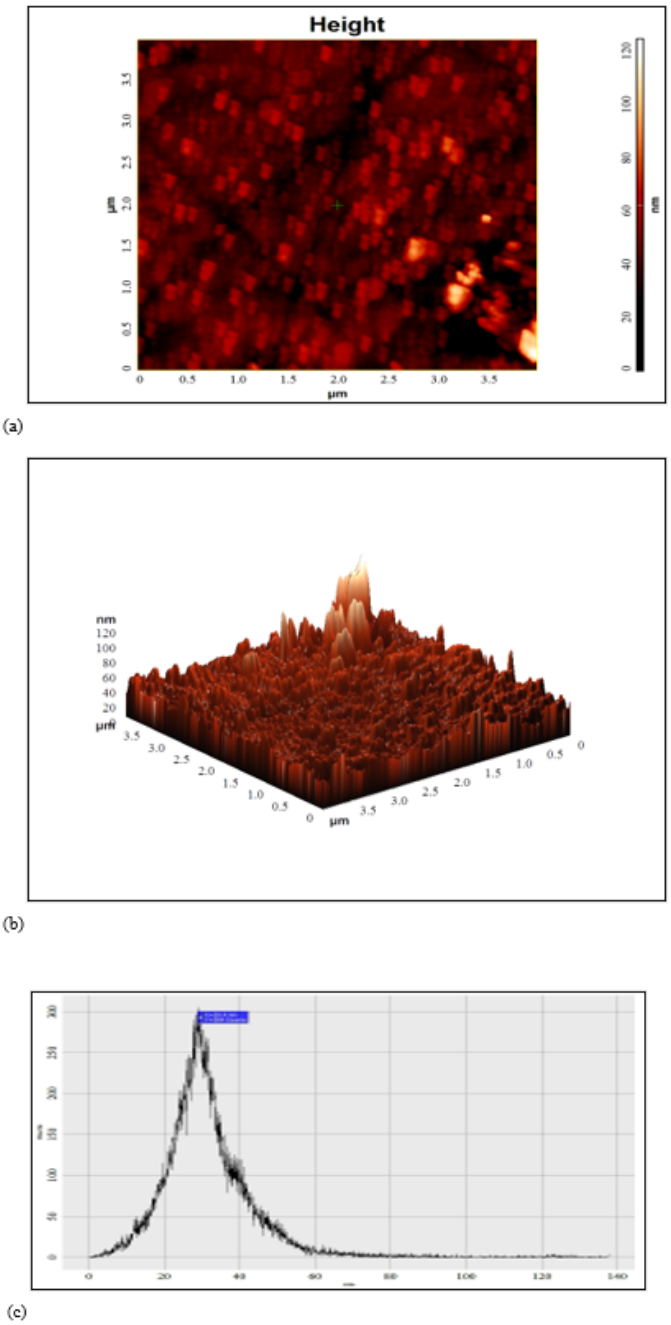

Max 137.714 nm.
Min 0 nm.
Eak-to-peak, Sy 137.714 nm.
Ten-point height, Sz 68.9463 nm.
Mean composite size: 29.4 nm.
Average 31.4881 nm.
Average roughness, Sa 8.27393 nm.
Root mean square, Sq 12.1479 nm

Figure 13: AFM study of (a) 2D image batch F5-Drug (b) 3D image of batch F5-drug and (c) Histogram of batch F5-drug.

The results of AFM study revealed that the after incorporation of drug in HA/CS composite the uniformity of composite size and shape was improved and had uniform shape of HA/CS-Drug composite (Batch F5).

Table 2: Results of Micrometrics Properties of HA/CS composites.

Batch	Mean composite size (μm)	Angle of repose (θ)	Hausner's ratio	Carr's index (%)	Porosity (%)
F1	35.06	33.54	1.36	26.53	20.48
F2	20.572	32.78	1.30	25.15	18.7
F3	11.765	26.18	1.28	24.92	19.02
F4	9.721	25.26	1.28	22.0	22.44
F5	3.892	22.06	1.21	17.99	26.53
F6	3.891	22.08	1.20	17.78	25.04

Table 3: Results of phosphorus ion concentration of Ha/CS composites.

Batch	Phosphorus ions concentration (mg/dL) in time (days)			
	1	3	5	8
F1	6.58	6	5.41	2.5
F2	7.35	7.33	6.08	5.08
F3	6.58	6.75	6.91	4.91
F4	14.6	14.08	14.33	11.91
F5	3.18	3.08	2.89	2.85
F5	6.58	6.33	5.75	2.5
Pure HA	9.33	8.5	8.08	8
SBF	5.37	5.34	5.33	5.33

DISCUSSION

The whole plant *T. cordifolia* is reported to possess antioxidant, antiarthritic, antidiabetic, anti- inflammatory, antiulcer, weakness, dyspepsia, fever, inflammation, jaundice, urinary, skin. Fascinatingly that the annual consumption of *T. cordifolia* in the Indian System of Medicines is 1,000 tonnes.[17-19] Initially we conducted simple extraction procedure to confirm the presence of berberine a biomarker compound of *T. cordifolia*. Further, we have determined the cytotoxicity of Amruth Mune a standardized extract of *T. cordifolia* on the RAW264.7 macrophages, the results ascertained that Amruth Mune did not show toxic effects on macrophages. Based on this, successive studies were conducted by choosing the safe medication dose of Amruth Mune i.e., 50 and 100 μg/mL.

NO was found to be a critical component of the immune system. There is evidence to support the secretion of NO by macrophages exhibited antipathogen and anti-tumor activity.[20,21] Therefore; NO measurement can reflect the effects of Amruth Mune on immune stimuli, which could be used as a quantitative marker of macrophage activation. Previous studies have reported that the various types of extracts of *T. cordifolia* are proved to enhance the phagocytic activity of macrophages, and it also increases the activation rate of macrophages.[22,23] The enhancement of phagocytosis is the distinctive feature of macrophage activation, the stimulation of macrophages enables the production of a variety of immunomodulatory

Substances involving cytokines, such as TNF-α and IL-6 triggering an array of innate immune responses to invading pathogens.[24]

In this study, Amruth Mune demonstrated macrophages stimulation and the effect was comparable with LPS, Amruth Mune enhanced the production of IL-1β and IL-6 in murine macrophages at the concentration of 100 μg/mL. These findings suggest that Amruth Mune had a strong immunomodulation effect on macrophages *in vitro*. Our results were coherent with the earlier published studies showing macrophage activation by LPS.[25] Understand the mechanism behind the activation of pro-inflammatory cytokines and increased production of NO. We evaluated effect of Amruth Mune on activation of MAPK signalling pathway. It has been reported that Mitogen Activated Protein Kinase (MAPK) plays a key role in innate and adoptive immune response.[26,27] Studies in connection with the immunomodulating materials reported they trigger macrophages via MAPK pathways.[28,29] In our investigation we also found that the phosphorylation of ERK, JNK and p38 upon treatment with Amruth Mune a standardized extract of *Tinospora cordifolia* which is almost equal to LPS, the above results revealed the molecular mechanisms of Amruth Mune in the activation of MAPK pathways in murine macrophages. Results were in line with previously published studies.[30,31]

CONCLUSION

While there are a number of approaches available as remedies for bone defects each with its own drawbacks, our formulation bypasses the majority of it making its more acceptable approach as treatment. Synthesized composites underwent to all required evaluation and characterization at every stage of formulation. Hence, assuring purity, absence of HA/CA interaction, F5 and F6 batch showing good correlation among all 6 batches, AFM reveling uniformity in composites size and shape and at last *in vitro* drug release study extending up to 12 hr where 92.32% release of drug was seen fulfilling all the checklist. To overcome the limitations of present medical procedures the research led to formation of nano-composites a novel approach for bone regeneration and bone tissue engineering.

ACKNOWLEDGEMENT

The authors would like to thank whole faculty members and management of the N.I.E.T (Pharmacy Institute), Greater Noida-201306 for providing all necessary technical supports and motivating us at every stage.

CONFLICT OF INTEREST

The authors declare that there is no conflict of interest.

ABBREVIATIONS

GERD: Gastroesophageal reflux disease; **P:** Pantoprazole; **PPI:** Proton pump inhibitors; **R:** Rebamipide; **H2RAs:** Histamine 2 receptor antagonists; **mg:** Milligram; **kg:** Kilogram; **i.e:** That is; **log:** Logarithm; **gm:** Gram.

REFERENCES

1. Chen J, Wang C, Lü S, Wu J, Guo X, Duan C, *et al*. *In vivo* chondrogenesis of adult bone-marrow-derived autologous mesenchymal stem cells. Cell Tissue Res. 2005;319(3):429-38. doi: 10.1007/s00441-004-1025-0, PMID 15672263.
2. Mishra G, Srivastava S, Nagori BP. Pharmacological and therapeutic activity of *Cissus quadrangularis*: an overview. Int J PharmTech Res CODEN. 1298–310;2(2).
3. Webster TJ. Nanotechnology for the regeneration of hard and soft tissues. Nanotechnol Regen Hard Soft Tissues. 2007:1-237.
4. Calderon L, Collin E, Velasco-Bayon D, Murphy M, O'Halloran D, Pandit A. Type II collagen-hyaluronan hydrogel-a step towards a scaffold for intervertebral disc tissue engineering. Eur Cell Mater. 2010;20:134-48. doi: 10.22203/ecm.v020a12, PMID 20821371.
5. Eibl R, Eibl D, Pörtner R, Catapano G, Czermak P. Cell and tissue reaction engineering. 2009 [cited Jul 25 2023]. Available from: http://link.springer.com/10.1007/978-3-540-68182-3.
6. Smith IO, Liu XH, Smith LA, Ma PX. Nanostructured polymer scaffolds for tissue engineering and regenerative medicine. Wiley Interdiscip Rev Nanomed Nanobiotechnol. 2009;1(2):226-36. doi: 10.1002/wnan.26, PMID 20049793.
7. Kaihara S, Borenstein J, Koka R, Lalan S, Ochoa ER, Ravens M, *et al.* Silicon micromachining to tissue engineer branched vascular channels for liver fabrication. Tissue Eng. 2000;6(2):105-17. doi: 10.1089/107632700320739, PMID 10941206.
8. Khademhosseini A, Langer R, Borenstein J, Vacanti JP. Microscale technologies for tissue engineering and biology. Proc Natl Acad Sci U S A. 2006;103(8):2480-7. doi: 10 .1073/pnas.0507681102, PMID 16477028.
9. Gunatillake PA, Adhikari R, Gadegaard N. Biodegradable synthetic polymers for tissue engineering. Eur Cell Mater. 2003;5:1-16; discussion 16. doi: 10.22203/ecm. v005a01, PMID 14562275.
10. Shahraki S, Shahbeiki F. Mohebbati* R. Investigating the cytotoxicity of the *Ziziphus jujuba* L. *Ribes khorasanicum, Crocus sativus* petal, and *Centella asiatica* extracts on the NIH/3T3 cell line. Herb Med J (Herb Med J). 2022;7(3).
11. Leitune VCB, Collares FM, Takimi A, Lima De GB, Petzhold CL, Bergmann CP, *et al.* Niobium pentoxide as a novel filler for dental adhesive resin. J Dent. 2013;41(2):106-13. doi: 10.1016/j.jdent.2012.04.022, PMID 22564371.
12. Malafaya PB, Silva GA, Reis RL. Natural-origin polymers as carriers and scaffolds for biomolecules and cell delivery in tissue engineering applications. Adv Drug Deliv Rev. 2007;59(4-5):207-33. doi: 10.1016/j.addr.2007.03.012, PMID 17482309.
13. Kumar PTS, Raj NM, Praveen G, Chennazhi KP, Nair SV, Jayakumar R. *In vitro* and *in vivo* evaluation of microporous chitosan hydrogel/nanofibrin composite bandage for skin tissue regeneration. Tissue Eng Part A. 2013;19(3-4):380-92. doi: 10.1089/ten. TEA.2012.0376, PMID 22934717. Available from: /pmc/articles/PMC3542877.
14. Nayak AK. Hydroxyapatite synthesis methodologies: an overview. Int J Chemtech Res CODEN; 2(2):903-7.
15. Nayak AK, Laha B, Sen KK. Development of hydroxyapatite-ciprofloxacin bone-implants using quality by design. Acta Pharm. 2011;61(1):25-36. doi: 10.2478 /v10007-011-0002-x, PMID 21406341.
16. Manuel CM, Ferraz MP, Monteiro FJ. Synthesis of hydroxyapatite and tricalcium phosphate nanoparticles-Preliminary studies. Key Eng Mater. 2003; 240-242: 555-8. doi: 10.4028/www.scientific.net/KEM.240-242.555.
17. Parkinson's Disease Foundation. Chitosan-hydroxyapatite composite biomaterials made by one step co-precipitation method: preparation, characterization and *in vivo* tests [internet] [cited Jul 25 2023]. Available from: https://www.researchgate.net/publication/ 291126418_Chitosan-hydroxyapatite_composite_biomaterials_made_by_one_ step_co-precipitation_method_preparation_characterization_and_*in_vivo*_tests.
18. Yu Y, Zhang H, Sun H, Xing D, Yao F. Nano-hydroxyapatite formation via co-precipitation with chitosan-g-poly(N-isopropylacrylamide) in coil and globule states for tissue engineering application. Front Chem Sci Eng. 2013;7(4):388-400. doi: 10.1007/s11705-013-1355-0.
19. Sivakumar M, Manjubala I, Panduranga Rao K. Preparation, characterization and *in vitro* release of gentamicin from coralline hydroxyapatite-chitosan composite microspheres. Carbohydr Polym. 2002;49(3):281-8. doi: 10.1016/ S0144-8617(01)00331-9.
20. Oyane A, Kim HM, Furuya T, Kokubo T, Miyazaki T, Nakamura T. Preparation and assessment of revised simulated body fluids. J Biomed Mater Res A. 2003;65(2):188-95. doi: 10.1002/jbm.a.10482, PMID 12734811.
21. Araújo LBDC, Silva SL, Galvão MAM, Ferreira MRA, Araújo EL, Randau KP, *et al.* Total phytosterol content in drug materials and extracts from roots of *Acanthospermum hispidum* by UV-vis spectrophotometry. Rev Bras Farmacognosia. 2013;23(5):736-42. doi: 10.1590/S0102-695X2013000500004.
22. Nikpour MR, Rabiee SM, Jahanshahi M. Synthesis and characterization of hydroxyapatite/chitosan nanocomposite materials for medical engineering applications. Compos B Eng. 2012;43(4):1881-6. doi: 10.1016/j. compositesb.2012.01.056.
23. Chen F, Wang ZC, Lin CJ. Preparation and characterization of nano-sized hydroxyapatite particles and hydroxyapatite/chitosan nano-composite for use in biomedical materials. Materials Letters. 2002;57(4):858-61. doi: 10.1016/ S0167-577X(02)00885-6.
24. Nikpour MR, Rabiee SM, Jahanshahi M. Synthesis and characterization of hydroxyapatite/chitosan nanocomposite materials for medical engineering applications. Compos B Eng. 2012;43(4):1881-6. doi: 10.1016/j. compositesb.2012.01.056.
25. Corcione CE, Frigione M. Characterization of nanocomposites by thermal analysis. Materials. 2012;5(12):2960-80. doi: 10.3390/ma5122960. Available from: /pmc/ articles/PMC5449060.
26. Venkatesan J, Qian ZJ, Ryu B, Ashok Kumar N, Kim SK. Preparation and characterization of carbon nanotube-grafted-chitosan - Natural hydroxyapatite composite for bone tissue engineering. Carbohydr Polym. 2011;83(2):569-77. doi: 10.1016/j.carbpol.2010.08.019.
27. Chesnutt BM, Viano AM, Yuan Y, Yang Y, Guda T, Appleford MR, *et al.* Design and characterization of a novel chitosan/nanocrystalline calcium phosphate composite scaffold for bone regeneration. J Biomed Mater Res A. 2009;88(2):491-502. doi: 10.1002/jbm.a.31878, PMID 18306307.
28. Tavakol S, Nikpour MR, Amani A, Soltani M, Rabiee SM, Rezayat SM, *et al.* Bone regeneration based on nano-hydroxyapatite and hydroxyapatite/chitosan nanocomposites: an *in vitro* and *in vivo* comparative study. J Nanopart Res. 2013;15(1). doi: 10.1007/s11051-012-1373-8.
29. Reves BT, Jennings JA, Bumgardner JD, Haggard WO. Preparation and functional assessment of composite chitosan-nano-hydroxyapatite scaffolds for bone regeneration. J Funct Biomater. 2012;3(1):114-30 [internet]. doi: 10.3390/jfb3010114, PMID 24956519.
30. Azami M, Tavakol S, Samadikuchaksaraei A, Hashjin MS, Baheiraei N, Kamali M, *et al.* A porous hydroxyapatite/gelatin nanocomposite scaffold for bone tissue repair:

in vitro and *in vivo* evaluation. J Biomater Sci Polym Ed. 2012;23(18):2353-68. doi: 10.1163/156856211X617713, PMID 22244095.

31. Le HR, Qu S, Mackay RE, Rothwell R. Fabrication and mechanical properties of chitosan composite membrane containing hydroxyapatite particles. J Adv Ceram. 2012;1(1):66-71. doi: 10.1007/s40145-012-0007-z.
32. Pallela R, Venkatesan J, Janapala VR, Kim SK. Biophysicochemical evaluation of chitosan-hydroxyapatite-marine sponge collagen composite for bone tissue engineering. J Biomed Mater Res A. 2012;100(2):486-95. doi: 10.1002/jbm.a.33292, PMID 22125128.

Cite this article: Patel TB, Padhiyar SP, Prajapati VT, Bhavsar VP, Patel ND, Shah DA. Preparation and Characterization of Hydroxyapatite-Chitosan Biocomposites of *Cissus quadrangularis* Linn. for Bone Regeneration in Osteoporosis. Int. J. Pharm. Investigation. 2024;14(1):212-24.